Synthesis and characterization of methacrylamide-based molecularly imprinted polymers for detection of di(2-ethylhexyl) phthalate

St Fauziah[1), *)] (ORCID ID:0000-0002-0599-4011), **Nunuk Hariani Soekamto**[1)] (0000-0001-8281-1752),
Paulina Taba[1)] (0000-0002-1266-5232), **Muralia Hustim**[2)] (0000-0001-8323-1549),
Annisyah Aprilia Achman[1)] (0009-0008-2915-4800), **Nital Andekan**[1)] (0009-0005-4425-5966),
Husnia Paraditha Husain[1)] (0009-0001-1716-5886), **Ajuk Sapar**[3)] (0000-0002-7278-6159)

DOI: https://doi.org/10.14314/polimery.2025.6.3

Abstract: Based on methacrylamide (MAM) and trimethylolpropane trimethacrylate (TRIM) as a cross-linking agent, molecularly imprinted polymers (MIPs) were obtained by precipitation polymerization and used for the detection of di(2-ethylhexyl)phthalate (DEHP) in drinking water in plastic packaging. The presence of functional groups –NH, –CH, –C=O, –C=C and –CO was confirmed by FT-IR. The formation of MIP_DEHP was also confirmed by EDS. Moreover, SAA analysis showed their mesoporous structure. The adsorption capacity was consistent with the isothermal Freundlich adsorption model, and the adsorption kinetics models with a pseudo-second-order reaction. Small, uniform, porous grains were observed in the MIP structure (SEM).

Keywords: polymer, phthalates, DEHP, methacrylamides, TRIM.

Synteza i charakterystyka polimerów na bazie metakryloamidu z nadrukiem molekularnym do wykrywania ftalanu di(2-etyloheksylu)

Streszczenie: Na bazie metakryloamidu (MAM) i trimetakrylanu trimetylopropanu (TRIM) jako środka sieciującego, metodą polimeryzacji strąceniowej, otrzymano polimery z nadrukiem molekularnym (MIP), które użyto do wykrywania di(2-etyloheksylo)ftalanu (DEHP) w wodzie pitnej w opakowaniach plastikowych. Obecność grup funkcyjnych –NH, –CH, –C=O, –C=C i –CO potwierdzono metodą FT-IR. Powstawanie MIP_DEHP potwierdzono również metodą EDS. Ponadto analiza SAA wykazała ich mezoporowatą strukturę. Pojemność adsorpcyjna była zgodna z izotermicznym modelem adsorpcji Freundlicha, a modele kinetyki adsorpcji z reakcją pseudodrugiego rzędu. W strukturze MIP zaobserwowano małe, jednolite, porowate ziarna (SEM).

Słowa kluczowe: polimer, ftalany, DEHP, metakryloamid, TRIM.

The widespread use of plastic, especially in beverage and food products, harms health. Plastic is made by adding phthalate compounds as plasticizers [1]. Phthalate compounds and their derivatives, such as di-2-ethylhexyl) phthalate (DEHP), are the main ingredients for making poly(ethylene terephthalate) (PET) plastic bottles [2]. DEHP compounds in PET bottles can migrate and dissolve in drinking water [2, 3] and cause reproductive and endocrine disorders [4, 5]. They are carcinogenic, harm human health, and are widely used as plasticizers for various packaging of food products, beverages [3], cosmetics, toys, and others. Therefore, it is necessary to analyze the presence of DEHP. MIP is the right adsorbent choice for detecting the presence of DEHP [6, 7]. MIPs with their active sites have high selectivity and affinity for target molecules and can be reused [8, 9]. According to Krisch (2000), MIP synthesis involves monomers, cross-linkers, initiators, template molecules, and porogen solvents [10]. One good monomer to use is methacrylamide monomer (MAM) [11]. Because of this, it is necessary to make a DEHP MIP based on MAM monomer to adsorb the DEHP target compound using types of cross-linkers, namely TRIM.

---

1) Department of Chemistry, Faculty of Mathematics and Natural Sciences, University of Hasanuddin, Makassar, 90245 Indonesia.

2) Department of Environmental Engineering, Faculty of Engineering, University of Hasanuddin, Makassar, 90245 Indonesia.

3) Department of Chemistry, Faculty of Mathematics and Natural Sciences, University of Tanjungpura, Pontianak, 78124 Indonesia.

*) Author for correspondence: stfauziah@unhas.ac.id

The aim of the work was to synthesize molecularly printed polymers (MIP) from methylacrylamide. Obtained MIP were characterized using Fourier transform infrared (FT-IR) spectroscopy, scanning electron microscopy (SEM), energy dispersive spectroscopy (EDS), surface area analysis (SAA) and ultraviolet-visible spectro-photometry (UV-Vis). Moreover, the ability to adsorb di(2-ethylhexyl) phthalate (DEHP) from water was also determined. This research is continuation of previously published research [12].

EXPERIMENTAL PART

Materials

DEHP 99.5%, methacrylamide 99% (MAM), trimethylolpropane trimethacrylate (TRIM), and azobisisobutyronitrile (AIBN) 75% were purchased from Sigma Aldrich (Saint Louis, MI, USA). Toluene PA, acetone PA, methanol PA, and acetic acid 96% PA were purchased from Merck (Darmstadt, Germany).

Synthesis of NIP and MIP_DEHP_MAM-*co*-TRIM

A total of 0.3945 mL (1 mmol) of DEHP was mixed with 0.3404 g (4 mmol) of MAM monomer into a round bottom flask and left for 5 min, and then added with TRIM crosslinker 2.5685 mL (8 mmol) and left for 5 min. After that, the mixture was added with 50 mL of toluene and prepolymerization occurred. The mixture was conducted sonication for 15 min, and oxygen was removed using N_2 gas for 10 min. Next, 1 mmol of AIBN initiator was added to the solution, then sonicated for 15 min and subjected to N_2. Furthermore, polymerization was conducted at 60°C on the water bath for 24 h [13]. The polymer formed was washed with distilled water, methanol, and acetone. Then, DEHP as a template molecule was extracted from the polymer by sonication using a solvent methanol and acetic acid with a ratio of 9:1 (v/v) for 30 min [14]. The polymer's name was MIP_DEHP_MAM-*co*-$\text{TRIM}_{(BE)}$ before extraction and MIP_DEHP_MAM-*co*-$\text{TRIM}_{(AE)}$ for extraction. The DEHP compounds in the extract were detected with a UV-Vis at a wavelength of 260 nm. This detection procedure is repeated until the extract absorbance value becomes zero where the DEHP has been extracted from the material. Next, wash the MIP with methanol and distilled water until the pH was neutral. Then, it is dried and further characterized. The synthesis of the non-imprinting polymer (NIP) was performed without DEHP, in the same manner as the MIP was prepared but without extraction. The polymer was named NIP_MAM-*co*-TRIM.

Methods

Ultra violet visible spectroscopy (UV-Vis) (Shimadzu UV-2600, Tokyo, Japan) was used to determine the amount of extracted DEHP at 260 nm. Fourier infrared spectroscopy (FT-IR) (Shimadzu IRPrestige-21, Tokyo, Japan) was used to analyze the chemical structure. The spectra were recorded using at least 32 scans with 2 cm^{-1} resolution, in the spectral range of 4000–350 cm^{-1}, using KBr pellets technique. The morphology and elements percentage were observed using a scanning electron microscope (JEOL JSM-6510 LA, Tokyo, Japan) and energy dispersive spectroscopy (EDS), respectively. A voltage of 10 kV and a magnification of 5000x were used. EDS measurements were performed using a current intensity of 1 nA, PHA T3 mode, real time 50.51 sec, lifetime 50 sec, idle time 1%, count rate 1349 cps and energy range 0–20 keV. The surface area was determined using surface area analyzer (Anton Paar NOVA 1200e, Graz, Austria). The volume and mean radius of pores were determined by the Barrett-Joyner-Halenda (BJH) method, and the surface area by the Brunauer-Emmett-Teller (BET) method. Both methods used the principle of nitrogen adsorption. The sample density was 1 g/cm^3.

Adsorption ability

30 mg of MIP_DEHP_MAM-*co*-TRIM and NIP were put into separate vials, then 5 mL of 15 mg/L of the DEHP solution was put into the vial. The mixture was stirred using a shaker for 1 h, and then filtered. The concentration of DEHP in the filtrate was analyzed using a spectrophotometer UV-Vis (Shimadzu UV-2600, Kyoto, Japan) at 252.6 nm wavelength. The DEHP amount adsorbed by MIP and NIP was calculated using Equation (1).

$$q_e = \frac{V(C_0 - C_e)}{m} \tag{1}$$

where: q_e is the amount adsorbed (mg/g), V is the solution volume (L), C_0 is the solution's initial concentration (mg/L), C_e is the solution's concentration after adsorption (mg/L), and m is the MIP mass (g) [15].

Effect of time on adsorption ability of DEHP by MIP

The amount of 5 mL of 15 mg/L DEHP standard solution and 30 mg of MIP_DEHP_MAM-*co*-TRIM were put into 5 vials. Next, the mixture was shaken using a shaker with varying times of 30, 90, 120, 150, and 180 min at 28°C. After adsorption was conducted at the specified time, the solution was filtered and then analyzed using a UV spectrophotometer at a wavelength of 252.6 nm [16].

Effect of concentration on adsorption ability of DEHP by MIP

A total of 5 mL of DEHP solution with different concentrations, namely 6, 9, 12, 18, and 21 mg/L at pH 6.8, was put into a vial containing 30 mg MIP_DEHP_MAM-*co*-TRIM each. The mixture was stirred with a shaker for 90 min at 28°C. Next, the solution was filtered and analyzed with a UV spectrophotometer at a wavelength of 252.6 nm [14].

Kinetics adsorption

The time effect analysis data was processed through the first-order pseudo-Equation 2, and the second-order pseudo-Equation 3 was used to determine the adsorption kinetics of MIP_DEHP_MAM-*co*-TRIM [16].

$$\ln(q_e - q_t) = \ln(q_e) - k_1 t \tag{2}$$

$$\frac{t}{q_t} = \frac{1}{k_2 q_e^2} + \frac{t}{q_e} \tag{3}$$

where q_e is the amount adsorbed at equilibrium (mg/g), q_t is the amount adsorbed at time t (mg/g), k_1 and k_2 are kinetic constant, t is time.

Adsorption capacity

The Langmuir isothermal adsorption equation (Eq. 2) and Freundlich isothermal (Eq. 3) were used to determine adsorption capacity from the concentration effect data [18].

RESULTS AND DISCUSSION

UV-Vis analysis

MIP_DEHP_MAM-*co*-TRIM was synthesized using a template molecule of DEHP, MAM monomer, and a crosslinker of TRIM by precipitation polymerization. The resulting MIP is a white, granular solid. DEHP compound in MIP was released using solvents like distilled water, methanol, and acetone, then extracted using a mixture of methanol: acetic acid (9:1 v/v) with sonication technique to produce MIP_DEHP_MAM. The extracted DEHP compound was evaluated qualitatively using UV-Vis at 260 nm, and the results can be seen in Table 1.

Table 1. UV-Vis results of DEHP in methanol extract: acetic acid (9:1)

Extracts number	Absorbance at 260 nm
E1	4.561
E2	3.453
E3	2.064
E4	1.107
E5	0.636
E6	0.573
E7	0.441
E8	0.209
E9	0.107
E10	0.065

The absorbance for each extraction repetition in Table 1 decreased from 4.561 to 0.065, which proves that DEHP has been extracted from MIP. The polymerization stages that occur in the synthesis of the MIP consist of pre-polymerization, polymerization, and extraction of DEHP from the MIP [19, 20]. The reaction scheme for the synthesis of MIP_DEHP_MAM-*co*-TRIM is presented in Figure 1. In the pre-polymerization stage (a), the DEHP template molecules and the MAM monomer first interact noncovalently and form hydrogen bond. In the polymerization stage (b), the TRIM and MAM form an MIP initiated by AIBN. The AIBN initiator has free radicals that can interact with the MAM monomer or TRIM crosslinker. Polymerization consists of initiation, propagation, and termination stages. The next stage is the extraction stage (c), where the DEHP is released from MIP and forms

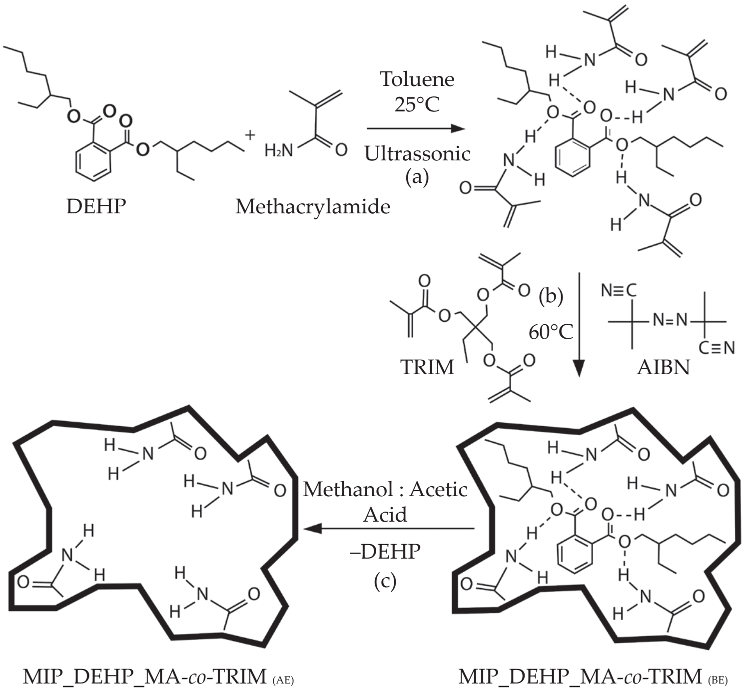

Fig. 1. Polymerization reaction of MIP_DEHP_MAM-*co*-TRIM extraction

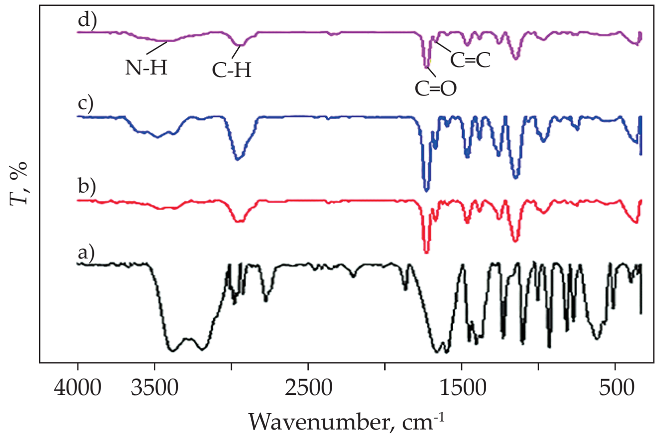

Fig. 2. FT-IR spectra: a) MAM b) NIP_MAM-*co*-TRIM, c) MIP_DEHP$_{(BE)}$, and d) MIP_DEHP$_{(AE)}$

a cavity or a mold with functional groups that match the target molecule (DEHP). DEHP can interact non-covalently via hydrogen bonds with the –CONH$_2$ functional group contained in MIP.

FT-IR analysis

FT-IR spectra are presented in Figure 2 and Table 2. MIP was formed from the interaction between MAM and TRIM, characterized by the presence of –NH, –C=O, –C=C, and –CH absorption and shifting in wave number and intensity change. The absorption band of –NH on NIP and MIP changes as the basicity of the monomer decreases after the polymer is formed. Table 2 shows that the –NH in the MIP_DEHP_MAM-*co*-TRIM$_{(BE)}$ and MIP_DEHP_MAM-*co*-TRIM$_{(AE)}$ materials undergo large wavenumber shift and stronger intensity. The –CH functional group in the three materials experiences a large wave number shift compared to MAM because –CH sp^2 in MAM undergoes addition to –CH sp^3. The functional group of –C=C in NIP_MAM-*co*-TRIM, MIP_DEHP_MAM-*co*-TRIM$_{(BE)}$, and MIP_DEHP_MAM-*co*-TRIM$_{(AE)}$ undergoing quite a large shift, and the –C=C intensity for the three materials was weaker than MAM. The interaction between the –NH group of MAM and –C=O in DEHP or MAM itself forms hydrogen bonds so that the functional group –C=O does not experience a change in the wave number for the materials NIP_MAM-*co*-TRIM, MIP_DEHP_MAM-*co*-TRIM$_{(BE)}$ and MIP_DEHP_ MA-*co*-TRIM$_{(AE)}$ when compared with MAM monomer. The bonds that play a role in the formation of NIP_MAM-*co*-TRIM and MIP_DEHP_MAM-*co*-TRIM are –NH, –C=C, –C=O, –CH, and C-H.

EDS and SEM analysis

The atomic composition of NIP_MAM-*co*-TRIM, MIP_DEHP_MAM-*co*-TRIM$_{(BE)}$, and MIP_DEHP_MAM-*co*-TRIM$_{(AE)}$, (C, O, N, and H atoms) was analyzed using EDS. The results are presented in Table 3. The mass of H atoms is impossible to detect because hydrogen atoms cannot be excited by X-rays, so EDS detectors cannot detect such low energy. The mass and atomic percent of C are used to prove the success of the MIP_DEHP_MAM-*co*-TRIM$_{(AE)}$ synthesis by looking at the magnitude of the loss of the mass percent of C and C atoms because DEHP is released from MIP.

The mass percentage of C and C atoms for MIP_DEHP_MAM-*co*-TRIM$_{(BE)}$ is higher than MIP_DEHP_MAM-*co*-TRIM$_{(AE)}$, whereas the mass percentage of O and O atoms for MIP_DEHP_MAM-*co*-TRIM$_{(BE)}$ is lower than MIP_DEHP_MAM-*co*-TRIM$_{(AE)}$. This is influenced by the number of C atoms in the DEHP compound, which is much more than the O atoms, so that when the DEHP compound is still in the polymer, the mass percent of C

T a b l e 2. FT-IR data of MAM, NIP_MAM-*co*-TRIM, MIP_DEHP$_{(BE)}$, and MIP_DEHP$_{(AE)}$

Functional groups	Wavenumber, cm^{-1}			
	MAM	NIP_MAM-*co*-TRIM	MIP_DEHP_MAM-*co*-TRIM$_{(BE)}$	MIP_DEHP_MAM-*co*-TRIM$_{(AE)}$
–NH stretching	3385; 3279	3468; 3374	3485; 3379	3464; 3381
–CH stretching	3100; 2928	3100; 2961	3100; 2961	3100; 2959
–C=O stretching	1667	1736	1736	1736
–C=C stretching	1603	1676	1680	1676

T a b l e 3. EDS data of NIP, MIP$_{(BE)}$ and MIP$_{(AE)}$

Elements	Mass, %			Atom, %		
	NIP	MIP $_{(BE)}$	MIP $_{(AE)}$	NIP	MIP $_{(BE)}$	MIP $_{(AE)}$
C	76.13	78.76	73.25	81.49	83.48	78.68
O	22.76	20.61	26.34	18.29	16.40	21.24

T a b l e 4. SAA results of MIP_DEHP_MAM-*co*-TRIM$_{(AE)}$

Sample	Surface area, m^2/g	Total pore volume, cm^3/g	Average pore radius, nm
MIP_DEHP_MAM-*co*-TRIM$_{(AE)}$	362.0731	0.4423	4.8892

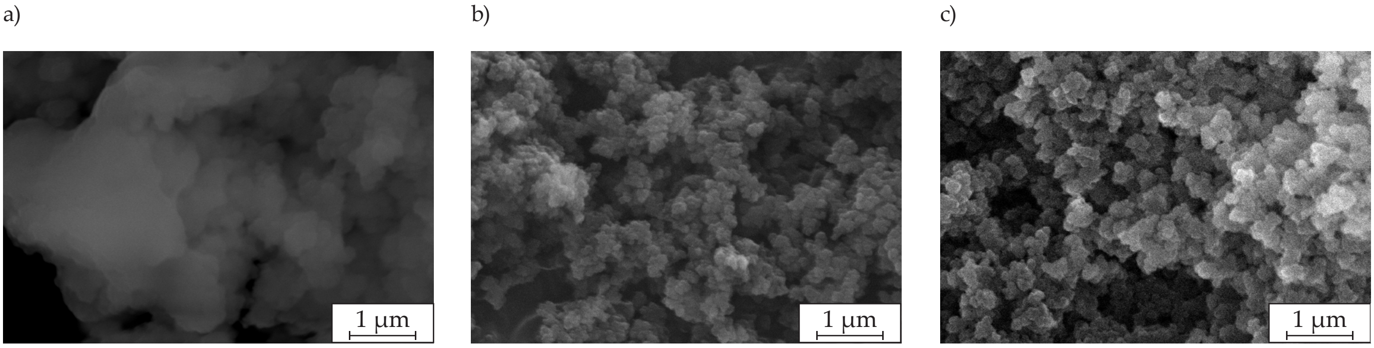

Fig. 3. SEM images: a) NIP_MAM-*co*-TRIM, b) MIP_DEHP_MAM-*co*-TRIM$_{(BE)}$, c) MIP_DEHP_MAM-*co*-TRIM$_{(AE)}$. 20,000× magnification

and C atoms increases, conversely when the DEHP compound has been released from the polymer the mass percent and O atoms increase. will increase, and the mass percentage of C and C atoms will decrease. The mass percentage of C and atomic percentage of C in MIP_DEHP_MAM-*co*-TRIM are 5.51% and 4.8%, respectively, and this shows that MIP has released DEHP. The mass percentage of C and atomic % of C in MIP decreased because the amount of DEHP in MIP was very small.

The surface morphology of NIP_MAM-*co*-TRIM, MIP_DEHP_MAM-*co*-TRIM$_{(BE)}$ and MIP_DEHP_MAM-*co*-TRIM$_{(AE)}$ were characterized using SEM as is shown in Figure 3.

SEM shows that the three polymers are in the form of granules with different grain size and density. NIP_MAM-*co*-TRIM (Fig. 3a) seems to consist of inhomogeneous and denser grains, MIP_DEHP_MAM-*co*-TRIM$_{(BE)}$ (Fig. 3b) seems to be homogeneous and less dense than NIP_MAM-*co*-TRIM, and MIP_DEHP_MAM-*co*-TRIM$_{(AE)}$ (Fig. 3c) is almost the same as MIP_DEHP_MAM-*co*-TRIM$_{(BE)}$, but MIP_DEHP_MAM-*co*-TRIM$_{(BE)}$ still seems to be more homogeneous than MIP_DEHP_MAM-*co*-TRIM$_{(AE)}$.

SAA analysis

Characterization using SAA with the Barret-Joyner-Halenda (BJH) method aims to determine the specific surface area, volume, and pore diameter of MIP and the pore diameter of MIP which is based on the results of isothermal adsorption at a very low temperature of 77.15 K and the amount of N_2 adsorbed by the sample. The results are presented in Table 4.

The MIP_DEHP_MAM-*co*-TRIM$_{(AE)}$ is categorized as mesoporous materials with an average pore radius size of 4.8892 nm. The IUPAC classifies material pore sizes, namely macropores (pore radius > 50 nm), mesopores (2 < pore radius < 50 nm), and micropores (pore radius < 2 nm) [20]. The pore volume total for a smaller size pore of 240.3667 nm is 0.4423 cm^3/g. Figure 4 displayed N_2 adsorption isothermal on MIP_DEHP_MAM-*co*-TRIM$_{(AE).}$

The lower curve in Figure 4 shows increasing adsorption time in the adsorption process, the volume increasing in relative pressure variation, while the upper curve is a desorption process with decreasing volume concerning variations in relative pressure. MIP_DEHP_MAM-*co*-TRIM$_{(AE)}$ can adsorb N_2 as much as 286.1125 cm^3/g at a relative pressure of 0.99. The BJH graph showing the pore distribution of MIP_DEHP_MAM-*co*-TRIM$_{(AE)}$ is presented in Figure 5.

The pore size distribution by the BJH method was obtained for an average pore radius ranging from 1.9 nm to 22.9 nm, which indicates its dominant distribution in the mesopore range. Figure 5 shows the pore distribution results for an average pore radius of 1.9 nm, which adsorbs up to 0.3597 cm^3/g N_2, and for an average pore radius of

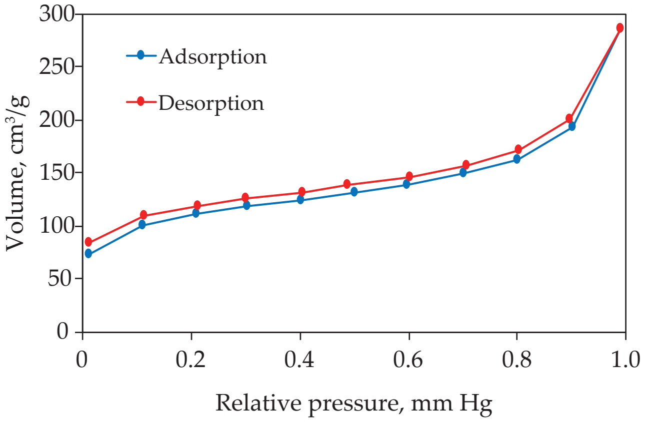

Fig. 4. Relationship between N_2 volume adsorbed on MIP_DEHP_MAM-*co*-TRIM$_{(AE)}$ and relative pressure

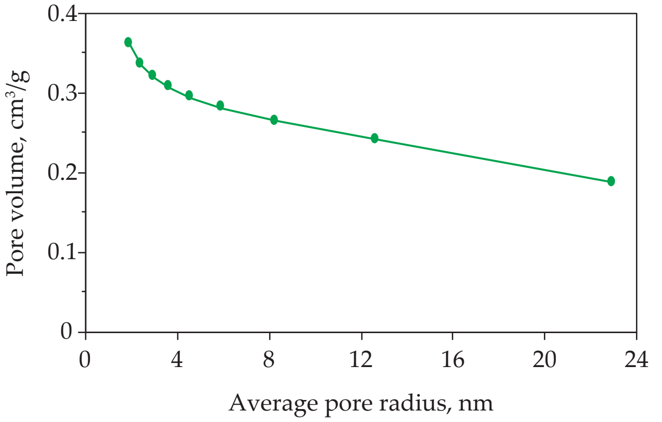

Fig. 5. Relationship between average pore radius and cumulative N_2 pore volume adsorbed on MIP_DEHP_MAM-*co*-TRIM$_{(AE)}$

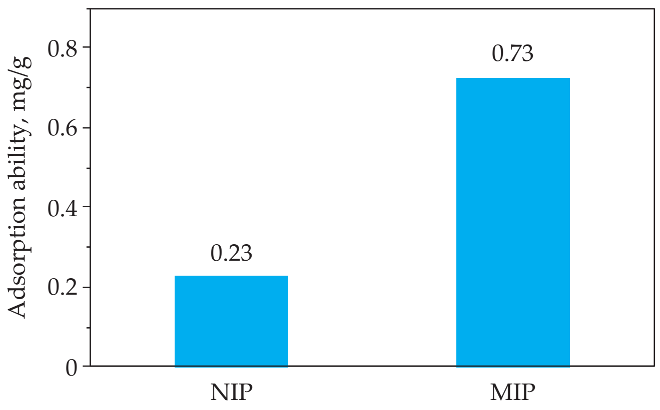

Fig. 6. Adsorption ability of NIP and MIP on DEHP

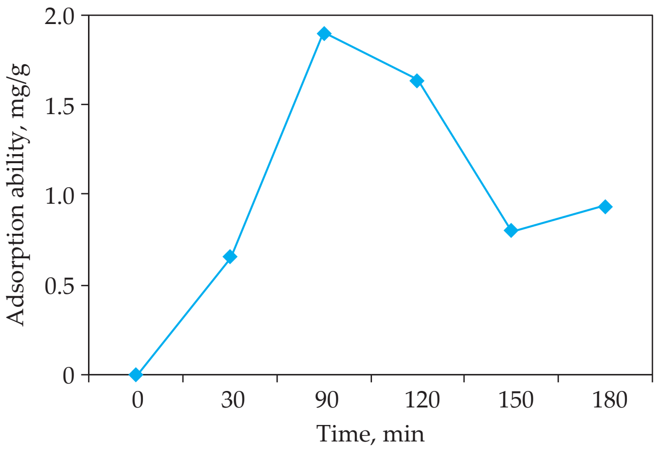

Fig. 7. Effect of time on the amount of DEHP adsorbed by MIP_DEHP_MAM-*co*-TRIM$_{(AE)}$

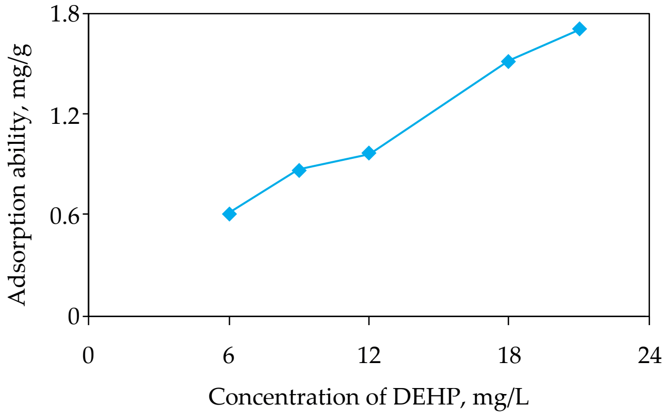

Fig. 8. Effect of concentration on the amount of DEHP adsorbed by MIP_DEHP_MAM-*co*-TRIM$_{(AE)}$

22.9 nm, which adsorbs up to 0.1871 cm^3/g N_2.This is following the results of BET analysis where all samples have an average pore radius in the mesopore range.

Adsorption ability

The adsorption capabilities of MIP_DEHP_MAM-*co*-TRIM$_{(AE)}$ and NIP_MAM-*co*-TRIM were tested. The good adsorption capabilities of the polymer were shown from the comparison of the amount of DEHP compounds adsorbed by MIP and NIP. Figure 6 displays the amount of DEHP compound adsorbed.

MIP material adsorbs DEHP compounds better than NIP, with a difference in the amount of DEHP adsorbed (Δqe) of 0.5 mg/g because MIP material has pores or cavities that correspond to DEHP molecules. Even though the adsorption performance of MIP material is better than NIP material, optimization with parameters of contact time and concentration needs to be carried out so that the maximum adsorption capacity can be determined.

Time effect of the adsorption ability of DEHP and DBP by MIP was conducted at different time intervals, which can be seen in Figure 7.

The quality of MIP material as an adsorbent can be determined through the time variable. The adsorbed DEHP compound increases with increasing contact time until it reaches maximum adsorption.

The best time for MIP_DEHP_MAM-*co*-TRIM$_{(AE)}$ to adsorb was 90 minutes with the amount of DEHP compound adsorbed as much as 1.89 mg/g. The MIP material is estimated to be saturated with DEHP compounds when maximum adsorption is reached. Further addition of time

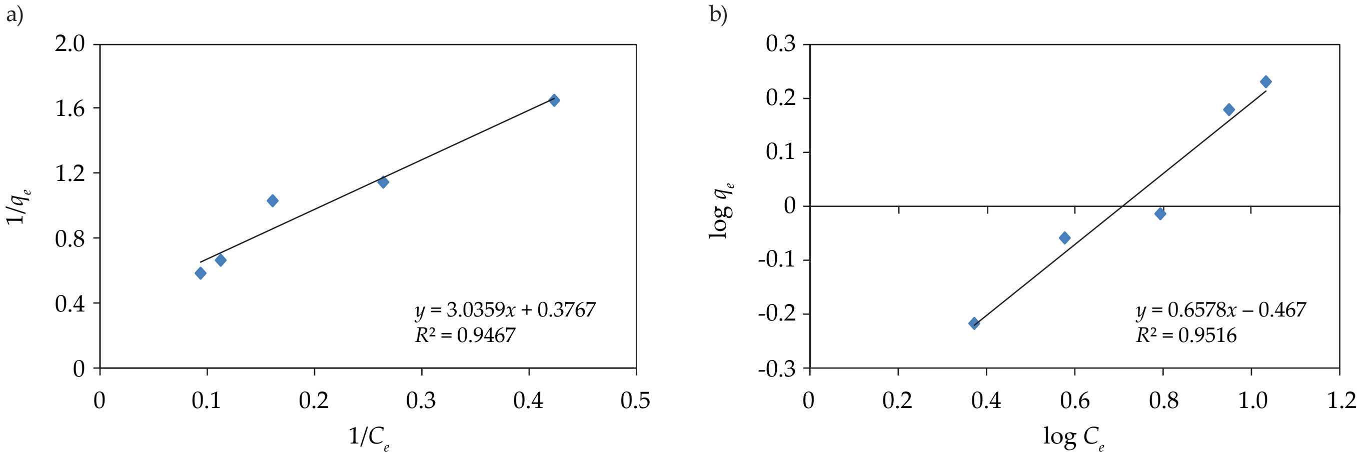

Fig. 9. DEHP adsorption isotherms by MIP_DEHP_MAM-*co*-TRIM(AE): a) Langmuir, b) Freundlich

T a b l e 5. DEHP adsorption parameters by MIP_DEHP_MAM-*co*-TRIM$_{(AE)}$

Sample	Isothermal adsorption Langmuir			Isothermal adsorption Freundlich		
	K_L	q_m, mg/g	R^2	K_F, mg/g	n	R^2
MIP_DEHP_MAM-*co*-TRIM$_{(AE)}$	0.1241	2.65	0.9467	0.34	1.52	0.9516

causes the adsorption ability to tend to decrease. The qe value increases at 180 minutes because the MIP material that is saturated with the DEHP compound will experience desorption, namely re-adsorbing the compound.

The effect of concentration on the adsorption of DEHP compounds by MIP is displayed in Figure 8.

The higher the initial concentration of the DEHP solution, the more DEHP compounds can be adsorbed by MIP_DEHP_MAM-*co*-TRIM$_{(AE)}$. The adsorption ability of MIP_DEHP_MAM-*co*-TRIM$_{(AE)}$ at the optimum material adsorption time (90 minutes) will increase when the concentration is increased and the maximum limit of adsorption equilibrium has been reached.

The adsorption capacity of MIP_DEHP_MAM-*co*-TRIM$_{(AE)}$ can be determined using the adsorption isothermal model of Langmuir and Freundlich. The linearity curve determines the suitability of the adsorption isothermal model. Langmuir and Freundlich adsorption isothermal curves are presented in Figure 9

The Langmuir adsorption isothermal linearity curve (Fig. 9a) is the relationship 1/qe and 1/Ce obtained from equation (3), while the Freundlich adsorption isothermal linearity curve is the relationship between log qe and log Ce obtained from Equation 4. Adsorption parameter data from each adsorption isothermal model is shown in Table 5.

The R^2 values for MIP_DEHP_MAM-*co*-TRIM$_{(AE)}$ in Figs. 9a and 9b are 0.9467 and 0.9516, respectively. The R^2 value of the Freundlich adsorption isothermal model is greater than the R^2 value of the Langmuir isothermal model. However, the R^2 values of both are close to each other, so it is necessary to create a non-linear curve to determine which adsorption isothermal model is most suitable for determining the adsorption capacity of the MIP_DEHP_MAM-*co*-TRIM$_{(AE)}$ material. The non-linear curve is presented in Figure 10.

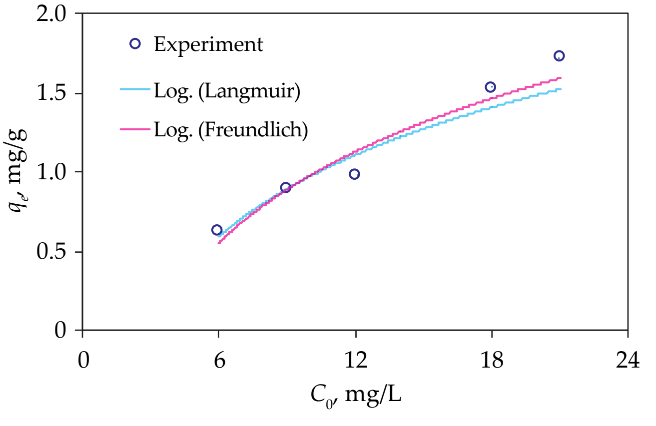

Fig. 10. Freundlich and Langmuir isothermal adsorption curves of MIP_DEHP_MAM-*co*-TRIM$_{(AE)}$

Based on Figure 10, it can be determined that Freundlich adsorption isothermal is more suitable than Langmuir adsorption isothermal. Therefore, the adsorption isotherm model of Freundlich was used to determine the adsorption capacity of MIP_DEHP_MAM-*co*-TRIM$_{(AE)}$ against DEHP.

Table 5 shows the adsorption capacity of MIP_DEHP_MAM-*co*-TRIM(AE) at KF of 0.34 mg/g. The adsorption intensity (n) of MIP_DEHP_MAM-*co*-TRIM(AE) is 1.52, which indicates that the adsorption of DEHP compounds by MIP_DEHP_MAM-*co*-TRIM(AE) is quite effective. The constant n is a constant describing the nature and strength of adsorption. The larger the value of n, the higher the adsorption strength. If $1 < n < 10$ then it shows highly effective absorption by MIP [22, 23].

CONCLUSIONS

NIP and MIP_DEHP_MAM-*co*-TRIM were successfully synthesized by precipitation polymerization method. FT-IR analysis showed the presence of functional groups –NH, –C=C, –C=O, –C–O and –C–H indicating the formation of NIP and MIP_DEHP polymers. The structure of the polymers shows small, uniform, and porous grains, which was confirmed by SEM. According to the SAA analysis, MIP can be classified as mesoporous polymers. The adsorption kinetics models are consistent with the pseudo-second-order adsorption model. The adsorption capacity of MIP_DEHP was consistent with the isothermal Freundlich adsorption model. It was also demonstrated that MIP_DEHP_MAM-*co*-TRIM is an effective DEHP compounds adsorbent and can be used to detect DEHP content in drinking water samples.

ACKNOWLEDGMENT

Thank you for the financial support of the Hasanuddin University Collaborative Fundamental Grant, Makassar, Indonesia (contract number 00309/UN4.22/PT.01.03/2024 for this research project.

Authors contribution

S.F. – conceptualization, investigation, , data curation, writing-original draft, funding acquisition; N.H.S. – formal analysis, writing-review and editing; P.T. – methodology, investigation; M.H. – writing-original draft, visualization,, writing-review and editing; A.A.A. – investigation, data curation; N.A. – investigation, data curation; H.P.H.: resources, investigation, project administration; A. S. – data curation, writing-original draft, writing-review and editing.

Funding

This project was funded by the Collaborative Fundamental Grant of Hasanuddin University, Makassar Indonesia (contract number 00309/UN4.22/PT.01.03/2024, 30 January 2024).

Conflict of interest

The authors declare no conflict of interest.

REFERENCES

[1] Kumari A., Kaur R.: *PeerJ* **2022**, *10*, e12859. https://doi.org/10.7717/peerj.12859

[2] Esteki F., Karimi H., Moazeni M. *et al.*: *Iranian Journal of Food Quality and Hazards Control* **2021**, *8(2)*, 66.

[3] Abdul Rasid H., Ungku Zainal Abidin UF., Jinap S. *et al.*: *Pertanika Journal of Tropical Agricultural Science* **2021**, *44(2)*, 389. https://doi.org/10.47836/pjtas.44.2.08

[4] Wang Y., Qian H.: *Healthcare* **2021**, *9(5)*, 603. https://doi.org/10.3390/healthcare9050603

[5] Prevarić V., Bureš M.S., Cvetnić M. *et al.*: *Chemical and Biochemical Engineering Quarterly* **2021**, *35(2)*, 81. https://doi.org/10.15255/CABEQ.2021.1928

[6] Yang Y., Yu J., Yin J. *et al.*: *Journal of Agricultural and Food Chemistry* **2014**, *62(46)*, 11130. https://doi.org/10.1021/jf5037933

[7] Vasapollo G., Del Sole R., Mergola L. *et al.*: *International Journal of Molecular Sciences* **2011**, *12(9)*, 5908. https://doi.org/10.3390/ijms12095908

[8] Hashemi-Moghaddam H., Rahimian M., Niromand B. *et al.*: *Bulletin of the Korean Chemical Society* **2013**, *34(8)*, 2330. http://doi.org/10.5012/bkcs.2013.34.8.2330

[9] Yulianti E.S., Rahman S.F., Whulanza Y. *et al.*: *Biosensors* **2022**, *12(12)*, 1090. https://doi.org/10.3390/bios12121090

[10] Yan H., Row K.H.: *International Journal of Molecular Sciences* **2006**, *7(5)*, 155. https://doi.org/10.3390/i7050155

[11] Fugolin A.P., Logan M.G., Kendall A.J. *et al.*: *Dental Materials* **2021**, *37(5)*, 805. https://doi.org/10.1016/j.dental.2021.02.004

[12] Fauziah S., Soekamto N.H.S., Budi P. *et al.*: *Polimery* **2023**, *68(7-8)*, 413. https://doi.org/10.14314/polimery.2022.7.7

[13] Tabarestani M.S., Rahnama K., Jahanshahi M. *et al.*: *Journal of Nanostructure* **2016**, *6(3)*, 245. https://doi.org/10.7508/JNS.2016.03.009

[14] Yang Z., Chen F., Tang Y. *et al.*: *Journal of the Chemical Society of Pakistan* **2015**, *37(5)*, 939.

[15] Zhou T., Tao Y., Jin H. *et al.*: *PLoS ONE* **2016**, *11(1)*, e0147002. https://doi.org/10.1371/journal.pone.0147002

[16] Tran H.N.: *Water*, **2023**, *15(6)*, 1231. https://doi.org/10.3390/w15061231

[17] Kostoglou M., Karapantsios T.D.: *Colloids and Interfaces* **2022**, *6(4)*, 55. https://doi.org/10.3390/colloids6040055

[18] Zhi K., Wang L., Zhang Y. *et al.*: *Journal of Molecular Recognition* **2018**, *31(3)*, e2627, https://doi.org/10.1002/jmr.2627

[19] Fauziah S., Magattang Gafur A., Soekamto N. *et al.*: *Egyptian Journal of Chemistry* **2021**, *64(5)*, 2385. https://doi.org/10.21608/ejchem.2021.44820.2912

[20] Hasanah A.N., Susanti I., Mutakin M.: *Molecules* **2022**, *27(9)*, 2880. https://doi.org/10.3390/molecules27092880

[21] Jung J., Park B., and Kim J. *et al.*: *Nanoscale Research Letters* **2012**, *7*, 34. https://doi.org/10.1186/1556-276X-7-34

[22] Amaly N., Istamboulie G., El-Moghazy A.Y. *et al.*: *Journal of Chemical Research* **2021**, *45(1-2)*, 102. https://doi.org/10.1177/1747519820925998

[23] Febrianto J., Kosasih A.N., Sunarso J. *et al.*: *Journal of Hazardeous Materials* **2009**, *162(2-3)*, 616. https://doi.org/10.1016/j.jhazmat.2008.06.042

Received 17 I 2025.
Accepted 19 II 2025.